Development of a quantitative PCR-High Resolution Melting assay for absolute measurement of coral-Symbiodiniaceae associations and its application to investigating variability at three spatial scales

Anne-Leila Meistertzheim, Xavier Pochon, Susanna A Wood, Jean-François Ghiglione, Laëtitia Hédouin

Development of a quantitative PCR-High Resolution Melting assay for absolute measurement of coral-Symbiodiniaceae associations and its application to investigating variability at three spatial scales

Anne-Leila Meistertzheim[1,2*], Xavier Pochon[3,4], Susanna A. Wood[3], Jean-François Ghiglione[2] and Laetitia Hédouin[1]

[1]Centre de Recherches Insulaires et Observatoire de l'Environnement, USR 3278 CNRS/EPHE/UPVD, Laboratoire d'Excellence "CORAIL", Université de Perpignan, 66860 Perpignan Cedex, France

[2]Sorbonne Universités, CNRS, UPMC Univ Paris 06, UMR 7621, Laboratoire d'Océanographie Microbienne, Observatoire Océanologique de Banyuls, Banyuls sur mer, France

[3]Coastal and Freshwater Group, Cawthron Institute, Private Bag 2, Nelson 7042, New Zealand

[4]Institute of Marine Science, University of Auckland, Private Bag 349, Warkworth 0941, New Zealand

Keywords

Absolute quantification; Endosymbionts; Holobiont; Symbiosis

****Corresponding author***

Anne-Leila Meistertzheim

Laboratoire d'océanographie microbienne (LOMIC) - UMR 7621 CNRS/UPMC, Station marine de l'UPMC - Laboratoire Arago, Avenue du Fontaule, 66650 Banyuls-sur-Mer, France

Tel: +334 68 88 73 01, Fax: +334 68 88 73 95, E-mail: anne-leila.meistertzheim@obs-banyuls.fr

Running title

Absolute quantification of endosymbionts in corals

Abstract

Previous molecular studies have shown that many corals host a dynamic consortium of dominant and background populations of Symbiodiniaceae genotypes with putatively distinct physiological traits. In the present study, we developed a quantitative PCR assay combined with High Resolution Melting analysis (qPCR-HRM) to distinguish which Symbiodiniaceae clades are present in a sample. Because the qPCR-HRM used in isolation yielded identical melt profiles for both clades A and C, this analysis was then coupled with further specific qPCR assays to enable the absolute quantification of all Symbiodiniaceae clades and host cells. When the assays were applied to *in hospite* samples, they had an absolute quantification level corresponding to one coral embryo of two cells and 1,000 symbiont cells. The assays were successful on coral fragments from twelve species (eight families). We then used the qPCR-HRM assay in an ecological survey of *Acropora pulchra* at different spatial scales (within colony, between colonies and between sites). Differences in abundance and composition of Symbiodiniaceae clades in *A. pulchra* were observed at all spatial scales, suggesting that various environmental factors drove changes in Symbiodiniaceae assemblages among and within coral colonies. The qPCR-HRM assay developed in this study is a relatively simple, cost-effective and reproducible tool that can be used to accurately differentiate and quantify endosymbiont Symbiodiniaceae clades in coral in the field. This will provide new insights into coral-symbiont shuffling mechanisms and the resilience of coral colonies to environmental stressors.

Introduction

Coral reefs provide niches for 25% of all marine species but occupy only 0.2% of the world's ocean surface area, and are therefore important hot spots of biodiversity (Reaka-Kudla 1997; Spalding and Grenfell 1997; Spalding et al. 2001). In nutrient poor environments, coral reefs depend on obligate symbiotic associations between corals and photosynthetic unicellular dinoflagellates in the family Symbiodiniaceae. This family is currently classified into nine divergent lineages, hereafter referred to as clades A to I (sensu Pochon and Gates 2010), of which seven have recently been elevated to genus level (Lajeunesse et al. 2018), and six are found in symbiosis with scleractinian corals (A–D, F and G;

Stat et al. 2008; Cooper et al. 2011a). Each Symbiodiniaceae clade encompasses significant within-clade genetic diversity (Pettay and Lajeunesse, 2013; Thornhill et al., 2017) corresponding to multiples species or types (Coffroth and Santos 2005). Experimental and field-based studies of coral bleaching events have shown that the physiology of the coral host is influenced by the genotypes of associated Symbiodiniaceae (Rowan 2004; Berkelmans and van Oppen 2006; Stat et al. 2006; Howells et al. 2012, 2013). For example, corals dominated by clade A symbionts were described as more prone to parasitism (Stat et al. 2008), whereas associations with clade C improved overall growth (Little et al. 2004; Cantin et al. 2009), and with type D1a (*Durusdinium trenchii* sensu LaJeunesse et al. 2018) thermo-tolerance was enhanced (Baker 2004; Stat and Gates 2011).

The association between a coral and several Symbiodiniaceae clades, often results in the presence of one dominant clade together with several background clades. The formation of partnerships between a coral and dominant Symbiodiniaceae clades often appears stable (Thornhill et al. 2009; LaJeunesse et al. 2010), and possibly driven by environmental conditions (Bongaerts et al. 2013; Tonk et al. 2014; Kennedy et al. 2016). However, the ability of corals to associate with multiple symbiont assemblages has been shown to be more widespread than previously reported (Silverstein et al. 2012).

The fragile symbiosis between corals and zooxanthellae is undergoing drastic changes due to shifting environmental conditions (Hughes et al. 2003; Hoegh-Guldberg et al. 2007). Rising seawater temperatures has led to an increase in stress-induced symbiosis breakdowns, also known as coral bleaching. Several massive coral bleaching events have been reported, resulting in a worldwide coral loss of 16% in 1998 (Wilkinson 2000). The most recent event was related to intense drought linked to El Niño (2015/2016), which resulted in the third worst worldwide mass bleaching event (National Oceanic and Atmospheric Administration [NOAA] Coral ReefWatch program 2016). The impact of this event is still incomplete but it is believed that it was the most severe coral bleaching event on record in the Great Barrier Reef (Hughes et al. 2017; NOAA Coral ReefWatch program 2017). During abnormally high seawater temperatures, certain coral species are more resistant to bleaching than others, and some bleached corals can recover (e.g. Jones et al. 2008). This observed resilience may be due to the capability

of some corals to 'switch' their symbionts (the uptake of more tolerant symbionts from the surrounding environment) or 'shuffle' their existing assemblage composition (background taxa may become abundant in higher temperatures; Baker 2003, 2004; LaJeunesse et al. 2009).

Few studies have investigated the impact of changes in background symbiont composition and density on coral stress resistance (e.g. Cunning and Baker 2012, 2014), and how this composition shifts after bleaching events (Cunning and Baker 2012; McGinley et al. 2012; Cunning et al. 2015a, 2016; Bay et al. 2016). It has been shown that the Symbiodiniaceae taxonomic composition may change within a coral colony (Ulstrup et al. 2007; Kemp et al. 2008, 2014). However, variation in absolute abundances (symbionts normalized to host parameters, such as units of DNA or cell numbers) of the nine Symbiodiniaceae clades remains unexplored. Development of a method to accurately measure absolute abundances of all nine Symbiodiniaceae clades would enable significant advancements in our understanding of the functional role of symbiont assemblages in coral symbiosis (Cunning and Baker 2014).

Quantitative PCR (qPCR) allows the description of the relative abundance of different symbiont clades, based on the number of copies of specific DNA loci within a sample (Ulstrup and Van Oppen 2003; Loram et al. 2007; Mieog et al. 2007). It has previously enabled the effective tracking of symbiont communities dynamics from five symbiont clades (A, B, C, D and F), that were standardized to host cells (Cunning and Baker 2012, Cunning et al., 2015a, Mieog et al. 2009). It has also enabled detection of low-abundance Symbiodiniaceae genotypes associated with corals (Silverstein et al. 2012; Rouzé et al. 2016) that were previously thought to harbor only a single dominant clade (Goulet 2007; but see Baker and Romanski 2007 and Mieog et al. 2007). However, absolute quantification of all Symbiodiniaceae clades had not yet been achieved because of; *i*) the lack of a robust and efficient DNA extraction method applicable to a wide range of sample types (cells/polyps, colonies, and replicate), *ii*) the inability of qPCR assays to target all clades (i.e. including clades G-I) and the absence of an internal-control for identifying missing clades (i.e., a family-Symbiodiniaceae target), and *iii*) the lack of qPCR amplification efficiency measurements amongst clades and single host cells.

A further benefit of qPCR is the ability to include High Resolution Melt curve to differentiate PCR products with different sequences. Two sequences containing at least one mutation generate fragments that rapidly denature and rejoin after PCR to form two (high-melting) homoduplexes and two (low-melting) heteroduplexes (base-pairing mismatches). The melting properties of these double-stranded PCR products are monitored through the release of a saturating fluorescent double stranded DNA binding dye as temperatures are increased, thus forming different melting curve shapes (Wittwer et al. 2003). Homozygous variants are therefore distinguishable from each other through differences in their melting temperature. We previously demonstrated that the identification of unknown specimens is undertaken by comparing these specimens to a set of reference melting curves (Meistertzheim et al. 2012).

The aim of this study was to develop an accurate, fast and highly reliable qPCR-High Resolution Melting (qPCR-HRM) assay that could be coupled with further qPCR assays to distinguish and quantify the nine Symbiodiniaceae clades in a wide range of coral taxa. For this purpose, we designed seven new clade-specific primer sets and one family-Symbiodiniaceae primer set, which were tested on a range of cultures and pure DNA samples from each of the nine existing Symbiodiniaceae clades. Additionally, two coral-specific (actin and nuclear ribosomal) primer sets were designed and used on Symbiodiniaceae-free embryos of *Acropora pulchra* to produce host standard curves for the quantification of coral cells. We validated our assay on colony fragments from twelve different species representing eight different families, and undertook an ecological survey of *A. pulchra* at different micro- and macro-scales (within colonies, between colonies and among sites).

Material and methods

Primer development

Alignment of 135 sequences of the nuclear large sub-unit ribosomal (28S) rRNA gene, including the 5' regions of the 5.8S and Internal Transcribed Spacer 2 (ITS2), were performed using MEGA6 (Tamura

et al. 2013). Seven clade-specific forward/reverse primer sets were designed using Primer Express v2.0 software (Applied Biosystems). The primers targeted an approximately 70-150 nucleotides [nt] region, one of the forward or reverse primer being located near the 3' end of the 5.8S rRNA gene or the 5' end of the 28S rRNA gene, and the corresponding reverse or forward primer being located in the ITS2 region (see Table 1). We also used previously published primers, including SYM_VAR_5.8S2 (Hume et al, 2015), and two actin primer sets specific to clades C and D (Cunning and Baker 2012). Host-specific (coral) primers were designed using alignments of the actin and nuclear 5.8S rDNA genes from GenBank (Table S1).

HRM analysis was used to quantify the number of clades present in each sample. This requires the amplification of a variable 80-nt partial sequence of the 5.8S gene using the forward SYM_VAR_5.8S2 and reverse Symb_R primer, hereafter referred to as the family primer pair 'Symb', which targets conserved flanked areas amplifying the nine different Symbiodiniaceae clades (Table 1; Figure S1). There are between one to ten mutations among clades in this gene (Table S2), which allows the distinction between them based on melting curve shape.

Absolute quantification assay development

Primer specificity was verified using DNA isolated from Symbiodiniaceae cell cultures in their vegetative state, from DNA collections of clades G-I (Table S3), and embryos of *A. pulchra*. Cells from Symbiodiniaceae-free embryos at division 2 and 4 cells were obtained following the procedure described in Hédouin et al. (2015), using *A. pulchra* colonies that were collected in September 2012 on the fringing reefs of Moorea Island (17° 30' S, 149° 50'W, French Polynesia, Society Archipelago, Figure 1 A-B).

We tested a new and automated extraction method, applicable to both coral embryos and polyps, which yields consistent DNA quantity between replicates and allowed successful DNA extraction from 2 cells for corals embryos. Symbiodiniaceae cultures, embryos and samples from coral colonies were lysed by mechanic action using the Y Matrix on a FastPrep Instrument (MP Biomedical, USA). Samples were

incubated with proteinase K (57°C, 1 hr). DNA was then isolated using a Maxwell® Blood DNA Purification Kit LEV (Promega, USA) on a Maxwell 16 MDx Instrument (Promega). DNA quality was assessed by electrophoresis on a 1% agarose gel. Total genomic DNA concentration were measured using spectrophotometry (Nanodrop ND-1000, Thermo Fisher scientific Inc., MA, USA).

Standard curves of Symbiodiniaceae and host cells were constructed to allow absolute quantification (Table S2). Living Symbiodiniaceae cells were quantified using a Scepter Handheld Automated Cell Counter system (Millipore, USA) combined with Scepter Pro software (Millipore). Automated cell counts were compared to cell counts obtained using a hemacytometer under a light microscope. DNA was extracted for each concentration as described previously. Standard curves were run in triplicate with cell concentrations of Symbiodiniaceae clades of 1×10^3 to 3×10^6 cells per DNA extraction (clades A-F), and using DNA concentrations ranging between 0.5 and about 40 ng DNA μL^{-1} (clades G, H and I). Two standard curves for the quantification of host-cells were run in triplicate using Symbiodiniaceae-free embryos with an increasing concentration of 2 to 400 cells per DNA extraction. *Acropora pulchra* were in their first and second division stages, and concentrations were determined by binocular microscopy.

Quantitative PCR reactions were performed in duplicate in a 10 µL volume containing genomic DNA, 1× High Resolution Melting master mix (Roche Diagnostics, USA) and 0.3 µM of each primer. The amplification protocol consisted of 10 min pre-incubation at 95ºC followed by 40 cycles of 95ºC for 15 s (ramp rate, 4.4 ºC. s^{-1}), touchdown annealing from 65 to 53 ºC for 15 s (ramp rate, 2.2 ºC s^{-1}), and extension at 72ºC for 20 s (s^{-1}ramp rate, 4.4 ºC. s^{-1}). The qPCR reactions were performed in 384-well plates using a LightCycler®480 Instrument (Roche Diagnostics, USA). After qPCR amplification, genotyping using HRM was undertaken. This consisted of a denaturing step at 95 ºC for 1 min, followed by a hybridization step at 40 ºC for 1 min. Melting curves were then constructed by ramping from 65 to 95ºC at 0.02ºC s^{-1}, taking 25 acquisitions of fluorescence measure per each degree centigrade. A negative (no-template) control was included in the PCR to detect potential DNA contamination or any formation

of primer dimers. Primer specificity was evaluated using qPCR analysis, gel electrophoresis and bi-directional sequencing of each positive qPCR product.

For each qPCR reaction, the crossing point (Cp; corresponding to the cycle threshold [Ct]) was determined using the "second derivative max method" implemented in the LightCycler®480 v.1.5.0 Software (Roche Diagnostics). The threshold for Ct calculation and normalization regions (leading and trailing ranges) for qPCR-HRM analysis were defined for each Symbiodiniaceae clade and host locus using serial dilutions of DNA and standard curves. Only successfully amplified samples with a Cp value within the linear part of the standard curves were considered for further analysis (Bustin et al. 2009). Individual qPCR efficiencies (E) of the Symbiodiniaceae clades and host reference genes were calculated using the formula: $E=10^{(-1/slope)}$, as described by Yuan et al. (2006). All primers had a qPCR efficiency between 1.84 and 2.02 (Table 1).

Conversion of quantification cycle values *Cp* into relative quantities Q_{clade_i} was undertaken for each DNA concentrations of the standard curves *i* using clade-specific primer pair using the modified equation described by Pfaffl (2001) without normalization by a reference gene:

$$Q_{clade_i} = E_{clade_i}^{\Delta Ct, clade_i}, \text{ (arbitrary unit)}$$

where E_{clade_i} is the amplification efficiency of the clade-specific primer couple *i* and ΔCt, $clade_i$ = Ct_{clade_i}(calibrator) - Ct_{clade_i} (sample).

The calibrator consisted of the maximal concentration of each Symbiodiniaceae clade included in the linear part of the standard curves.

The Q_{clade_i} was calculated for each DNA concentrations in nanograms (ng) from the linear part of each standard curve *i*, allowing the derivation of the following equation:

$$DNA_{clade_i} = f\left(Q_{clade_i}\right) \text{ (ng)}$$

Similarly, the family primer pair 'Symb' was used to amplify total DNA copies of Symbiodiniaceae in one reaction such that:

$Q_{TotSymb} = E_{Symb}^{\Delta Ct,Symb}$, (arbitrary unit)

The $Q_{TotSymb}$ was then calculated for each DNA concentrations from the Symbiodiniaceae standard curves, subsequently allowing for the derivation of the following equation:

$DNA_{TotSymb} = f(Q_{TotSymb})$ (ng)

These standard curves allowed for the concentrations of each clade *i* and total Symbiodiniaceae (per cell or DNA unit) of the unknown samples to be determined (Pfaffl, 2004). We considered this method as sufficiently accurate when $DNA_{Symb} = \sum_{i=1}^{9} DNA_{clade_i}$ (ng).

The quantity of host cells was calculated using the two Q_{ref_i} calculated as described above from the two host reference genes. The calculated values were plotted against the linear regression of each corresponding standard curve, where:

$Q_{ref_i} = E_{ref_i}^{\Delta Ct,ref_i}$, (arbitrary unit)

Finally, the concentration of host cells was assessed by the geometric mean of the Q_{ref_i} such as described by Hellemans et al., (2007) to normalize relative quantities with multiple reference genes:

$$Q_{Host} = \sqrt{\prod_{i}^{2} Q_{ref_i}}$$

The Q_{Host} was then calculated for each DNA concentrations from the host standard curves, subsequently allowing for the derivation of the following equation:

DNA_{Host} = f(Q_{Host}) (ng).

Finally, the linear part of each standard curve allowed for the quantification of both Symbiodiniaceae and its host using specific and family primers starting from a known quantity of DNA, such that

$DNA_{Reaction} = DNA_{Host} + DNA_{Symb}$ (ng)

and

$$DNA_{Reaction} = DNA_{Host} + \sum_{i=1}^{9} DNA_{clade_i} \text{ (ng)}$$

The HRM data obtained with the family-Symbiodiniaceae primers 'Symb' resulted in differences in curve shapes for each Symbiodiniaceae clade which were discriminated using the Gene Scanning module of the LightCycler 480 v.1.5.0 Software (Roche Diagnostics, USA). Melting curve data was adjusted manually as previously described (Meistertzheim et al. 2012), and normalized fluorescence conditions were established and adjusted, with the threshold set to 0 and the sensitivity at 0.26 (Lavergne et al. 2014). Curve shapes and Tm were compared between samples of the same clade and between clades. Shape similarities or differences in the melting curves between samples were assessed visually and mathematically by calculating the root-mean square error (RMSE) values. The latter were calculated by pairwise comparison of the normalized fluorescence data of melting curves obtained for each Symbiodiniaceae clade as recommended by Naue et al. (2014). The intra- and inter-run accuracy of HRM results were estimated by calculating the RMSE values of three runs of triplicate amplifications of all standard curves. The influence of template DNA was also investigated for each Symbiodiniaceae clade and embryos of *A. pulchra* at a DNA concentration range between 100 pg and 500 ng. Finally, to confirm the number of clades present in one sample by HRM, DNA from various clades was mixed in different proportions to obtain reference melting curves of DNA mixtures. DNA from clades A-D, F and G were cross-mixed in pairs using three different proportions of DNA (25:75, 50:50, 75:25) and by using three to five clades combined at equimolar proportion, and at a final DNA concentration of 15 ng DNA μL^{-1}.

Validation test of host quantification using other coral species

We then tested the applicability of only the two coral reference genes to be applied to species other than *A. pulchra* because the other primer sets will target Symbiodiniaceae clades whatever the host species.

Of the 67 scleractinian species from nine different families previously described in Moorea Island (Bosserelle et al. 2014), twelve species representing eight different families were chosen, including Acroporidae (*Acropora pulchra, Astreopora* sp. and *Montipora capitata*), Agariciidae (*Pachyseris speciosa* and *Pavona cactus*), Faviidae (*Dipsastraea [Favia] stelligera*), Fungiidae (*Danafungia* sp.), Merulinidae (*Cyphastrea serailia*), Pocilloporidae (*Pocillopora damicornis*), Poritidae (*Porites rus* and *Napopora irregularis*) and Psammocoridae (*Psammocora contigua*).

Two or three colony fragments (ca. 0.5-1 cm^2) of the coral species were sampled by diving in several reef sites of Moorea and Tahiti Islands. The coral fragments were collected using wire cutters and clamps previously cleaned with sodium hydroxide and ethanol to avoid cross-contamination between samples. Each fragment was collected from the tip of each coral and fixed separately in 70% ethanol.

Coral samples were washed in DNAse-free water before performing DNA extraction, as described above. DNA was diluted to 15 ng μL^{-1} and 30 ng was used to conduct qPCR-HRM assays. To ensure replicability and homogeneity, each plate contained DNA from a representative of the nine Symbiodiniaceae clades in duplicate, as well as Symbiodiniaceae-free coral embryos and a negative control.

Comparison of Symbiodiniaceae assemblages in Acropora pulchra at micro and macro-scale

Twenty colonies of *A. pulchra* were collected in September 2012 from Mahana (17°29'18"S; 149°53'7"W) and Teavaro (17°30'23"S; 149°45'53"W), two fringing reef sites in Moorea Island (Figure 1). These two sites were chosen because *A. pulchra* colonies were found in high abundances at both sites despite contrasting turbidity (0.12 *vs* 0.04 NTU in Mahana and Teavaro sites, respectively). Turbidity, salinity, temperature, and pH were recorded using the multiparameter HORIBA U50 probe. To examine the spatial distribution of symbiont clades within a host colony, branch fragments (approximately 0.5-1 cm^2) were sampled using individual sterilized wire cutters and clamps. Coral samples were collected on both the upward and downward facing sides of coral branches, exhibiting

two distinct color morphs (normal [N] and slightly bleached [sB]), representing different micro-variation of the environment; Figure 1C-E). These were preserved in 70% ethanol and stored at -20°C until DNA extraction. DNA extractions were undertaken as described above. Absolute quantification by qPCR assay and HRM was undertaken in duplicate using standard curves of Symbiodiniaceae clades and *A. pulchra* embryos with a no-template control in each plate.

Tests for normality and homoscedasticity on obtained DNA concentrations were performed using the Statistica software v10 (Statsoft) using Shapiro-Wilk and Levene tests. Concentration differences between coral-color fragments and sites for the number of host-cells, total Symbiodiniaceae cells, and cell counts for each specific Symbiodiniaceae clade were compared using non-parametric Kruskal-Wallis and Mann-Whitney *U*-tests.

Results

Quantification of symbiont and host cells

Standard curves generated from increasing Symbiodiniaceae cells ranging from $1x10^3$ to $3x10^6$ cells per extraction resulted in DNA ranging concentrations of 1 to 200 ng DNA μL^{-1}. For all clades, there was a strong correlation between the DNA concentrations and the cell numbers with correlation coefficient R^2 higher than 0.95 (e.g., for clade C R^2=0.96 ± 0.03 SD; Figure S2A). Linear curves were obtained for host cell, with DNA concentrations gradually increasing (9 to 670 ng DNA μL^{-1}) as the number of host cells per extraction rose from 2 to 400 (R^2=0.996 ± 0.004, Figure S2B). Using qPCR analysis, quantification of the total number of Symbiodiniaceae cells was performed using the family primer pair 'Symb' with DNA extracted from 1×10^3 to 3×10^6 cells per extraction of all individual clades (Table S4). The resulting standard curves obtained for each clade ($DNA_{TotSymb} = f(Q_{TotSymb})$) indicated high correlation coefficients (mean R^2=0.96 ± 0.04; Figure 2A for clade C). The clade-specific Symbiodiniaceae primers, also had standard curves ($DNA_{clade_i} = f(Q_{clade_i})$) with high coefficient correlation values (mean R^2=0.96 ± 0.04; Figure 2A for clade C and Table S4). We obtained similar

specificity and efficiency (E_{Symb}) for qPCR amplifications tested on representative samples from each of the nine clades using the family primers 'Symb' (Table S5), suggesting that these loci are conserved within Symbiodiniaceae lineages. Host standard curves, which allowed for the quantification of polyp cells, were constructed (2 to 200 cells; Figure 2B) with the highest accuracy obtained between 2 and 50 cells (R^2=0.98 ± 0.02), corresponding to DNA concentrations ranging between 10 and 90 ng DNA μL^{-1} (Figure S2B). No DNA amplification was obtained from embryos cells when using primers designed for Symbiodiniaceae, or from dinoflagellates cells when using primers designed for host genes. Duplicates produced gap values between both Ct lower than 0.5.

Reproducibility, accuracy and specificity of the High Resolution Melt curve genotyping

The HRM assay using the family locus of 5.8S rDNA for the entire genus Symbiodiniaceae allowed for correct discrimination between all clades except clades A and C when compared to the selected cell cultures and DNA collection (Table S2). Discrimination was explored by visual inspection of the melting curves (Figure 3A and 3B) and by calculating RMSE values (Figure 3C). The visual and mathematical distinction between clades was clearly visible for all Symbiodiniaceae lineages explored in this study, except for clades A and C. However, when different clades are co-occurring, the method effectively detected the presence of heteroduplexes (e.g. AC; see below). Symbiodiniaceae identification by HRM using the family-specific primer pair (Symb) on material derived from cell cultures always corroborated the results from clade-specific primers. The Tm of all analyzed samples ranged between 82°C and 84°C (Figure 3A). Seven clades were easily identifiable and the mean RMSE values for comparisons of samples from the nine clades (Figure 3C) ranged from 2.70 (±0.16) to 32.56 (±0.03), corresponding to the number of mutations (1-13, Table S3). The lowest RMSE values were obtained when comparing clades A and C (mean 0.84 ± 0.09), whose sequences differed by five mutations (Table 2). Although up to two mutations were present within the reverse (*Symb*R) primer region (Figure S1), similar amplification efficiencies were obtained using the family primer in the clade-specific standard curves (Figure 2), highlighting similar amplification efficiencies between clades

(Table S5). No DNA amplification was obtained from our negative controls. Nine replicate reactions per clade and per experimental run, including standard curves of cell cultures and triplicate DNA samples, yielded similar Ct values ($\Delta Ct < 0.5$) and similar melting curves corresponding to low RMSE for intra- and inter-run comparisons (mean values of 1.0 ± 0.3 and 2.2 ± 0.6, respectively). Similar melting curve shapes were obtained among sub-clade genotypes (Table S2) within five clades (A, B, F, G and H), with RMSE values intra-clades ranging from 0.09 to 2.12 (mean value of 1.25 ± 0.46) (Table S5).

Limits of the High Resolution Melt curve method and application to coral tissue samples

We obtained similar melting curve shapes for the nine Symbiodiniaceae clades, with DNA concentrations ranging from 100 pg to 500 ng and a mean RMSE value of 0.68 ± 0.37. It indicated that low template DNA concentration did not significant change the melting curve shapes. Melting curves obtained using experimental mixtures of pairwise clade DNA comparisons (using mixed combinations among clades A, B, C, D and F) always displayed more than two peaks, including the mixture of A and C, thus confirming the presence of two different DNA amplifications and their corresponding homoduplexes and heteroduplexes in the reaction (Figure 4A). DNA mixed in the same proportions using three, four and/or five clades always yielded melting curve shapes with three peaks regardless of the proportions used (Figure 4B), confirming the presence of three or more clades in a reaction which was further validated by three or more positive amplifications using the specific primers. However, the intensity of both peaks changed when applying variable proportions of two clades (Figure 4C).

The method assumes that the copy number of the locus targeted by the qPCR primers is the same within each clade. However, further investigations are required whether this assumption is valid and can be applied to the absolute quantification of all clades in coral samples.

Validation tests of host quantification using other coral species

For the twelve coral species, amplifications of the host DNA using the host-specific primer sets were positive regardless of the coral species investigated in this study. The Cp values of the host primer set (host genes) always fell within the constructed standard curves using *A. pulchra* embryos, i.e. less than 30 PCR cycles (data not shown).

Field survey of Acropora pulchra at micro and macro-scales

We analyzed a total of 40 fragments of *A. pulchra* collected from two sites (Mahana and Teavaro) and including two distinct color morphs. Out of the nine existing Symbiodiniaceae clades, only three (A, C, and D) were detected using the qPCR-HRM assay (Figures 5 and 6). Colonies showed significantly higher concentrations of total Symbiodiniaceae DNA per total DNA in Mahana compared to Teavaro (mean of $DNA_{TotSymb}$ ± SD = 12.1% ± 3.0%, and 7.1% ± 1.3%, respectively, Mann-Whitney *U*-test, $p<0.001$). The values were similar between the normal and slightly bleached coral fragments within a site (Figure 5). Concentrations of clade A cells were 2-fold higher in colonies from Mahana compared to Teavaro (mean 6.5% ± 1.6% and 2.7% ± 0.4%, respectively; Mann-Whitney *U*-test, $p<0.001$). Clade C cells were identified almost exclusively in colonies from Teavaro at a mean concentration of 7% ± 1%, except for two colonies in Mahana with medium color loss (Figure 6). For these two colonies, fragments collected from a branch (above *vs* below) harbored different proportions of Symbiodiniaceae (8.2% *vs* 5.4%, 0% *vs* 3.0% and 5.6% *vs* 2.6%, for clades A, C and D, respectively, Figure 6). In contrast, clade D cells were detected exclusively from Mahana colonies (mean 4.8% ± 2.6%).

Discussion

Quantitative PCR-High Resolution Melt assay

This study developed a new qPCR-HRM assay to explore Symbiodiniaceae clades present in a coral fragment smaller than 1 cm^2. This assay was coupled with further clade and host specific assays and allowed, for the first time, the absolute quantification of the proportions of each Symbiodiniaceae clade

384 in coral tissues normalized by the number of host cells. This quantification was based on standard curves
385 generated using Symbiodiniaceae-free coral cells and representative DNA or cultures from each of the
386 nine existing clades, the latter being haploid in vegetative stage in both cultured and *in hospite* (Santos
387 and Coffroth 2003). The method assumes that copy number of the locus targeted by the qPCR primers
388 is the same in the cells used as the standard curve template and the cells present in the unknown sample
389 (within each clade). This allows for the establishment of a correlative relationship between the number
390 of living cells in each clade and qPCR values. However, additional research is required to confirm this
391 assumption.

392 The qPCR-HRM assay developed in the present study provides a simple way to identify which
393 clades are present in mixed environmental samples. Granados-Cifuentes and Rodriguez-Lanetty (2011)
394 showed that HRM is a more effective option, than relatively time-consuming molecular fingerprinting
395 methods such as Denaturing Gradient Gel Electrophoresis for identifying mixed-clade combinations.
396 Our results demonstrated that HRM is able to identify each Symbiodiniaceae clade in isolation but failed
397 to differentiate clades A and C due to their identical melting curves. Two amplicons can have the same
398 melting behavior despite sequences not being exactly the same, e.g., due to an erasing effect caused by
399 two mutations (e.g. T to G and G to T) (Druml and Cichna-Markl 2014). However, the present study
400 also demonstrated that when different clades are mixed together, including the mixing of A and C,
401 heteroduplexes are always produced which are easily detectable by HRM because they alter the shape
402 of the melting curves (Wittwer et al. 2003). Our HRM results were also corroborated by clade-specific
403 qPCR amplifications. By combining HRM with qPCR, we gained insights into the absolute
404 quantification of the coral polyp and its symbiont cladal content. Quantitative PCR analyses has
405 previously been described as a powerful method for quantifying Symbiodiniaceae clades A-F (Loram et
406 al. 2007; Mieog et al. 2007; Bay et al. 2016; Rouzé et al. 2016, 2017). These studies quantified the
407 relative proportion of PCR amplicons from each symbiotic clade, standardizing their assays using a
408 single host gene. However, there was no in-depth assessment of the potential effect additional clades
409 (i.e., G, H, and I) may have on the overall assay. Furthermore, differential efficiencies of PCR
410 amplification among clades and host cells were not taken into account possibly leading to an

411 underestimation of clade proportions. These assays also lacked total Symbiodiniaceae cell internal
412 controls. The assay described in the present study quantifies host cells through amplification of two
413 conserved reference host genes, and we showed that this could be applied to twelve coral species
414 representing eight different coral families. Using specific and family primers of the nine
415 Symbiodiniaceae clades and two host genes to construct standard curves of symbiotic and host cells, our
416 method quantifies the total abundance of Symbiodiniaceae and each specific clade composition,
417 normalized per host parameters, in terms of DNA values (in nanograms) or cell numbers, as previously
418 recommended (Cunning and Baker 2014).

419

420 *Limitations*

421 Using high concentrations of DNA can lead to misidentification of clades when using qPCR-HRM
422 assays (Granados-Cifuentes and Rodriguez-Lanetty 2011). In the present study, the upper limit of DNA
423 templates for the assay was not reached with maximal values of DNA for embryos at 670 $ng.\mu L^{-1}$ and
424 Symbiodiniaceae at 200 $ng.\mu L^{-1}$. We also obtained accurate and reproducible results with 30 ng of total
425 DNA extracted from each coral fragment. The lower limit of the method corresponded to one embryo
426 of two cells, and to 10^3 cells of Symbiodiniaceae. This limit is lower than population sizes measured
427 within planulae ($7.4.10^4$ in 1 mm long; Marshall 1932) or within individual fragments of coral colony
428 ($\sim 10^6$ cells cm^{-2}; Fitt et al. 2000). This method is therefore particularly useful for accurately detecting
429 background Symbiodiniaceae clades within a sample. Unlike High-Throughput Sequencing (HTS)
430 methods (Arif et al. 2014; Edmunds et al. 2014; Quigley et al. 2014; Thomas et al. 2014; Boulotte et al.
431 2016; Hume et al. 2018), our assay is unable to provide information on the total genetic diversity of
432 within-clade assemblages. Nevertheless, HTS methods are relatively costly and time-consuming
433 compared to the qPCR-HRM method presented here, which requires fewer processing steps and
434 produces results within hours and at relatively low cost. This method may effectively complement HTS
435 studies when dealing with large numbers of small individual samples (Cousins et al. 2012; Cristescu
436 2014).

437

438 *Endosymbiotic Symbiodiniaceae genotypes composition of Acropora pulchra at different spatial scales*

439 The ecological role of dominant Symbiodiniaceae genotypes in coral host physiology and stress
440 tolerance has been extensively studied (Rowan and Knowlton 1995; Baker 2003; Coffroth and Santos
441 2005; Stat et al. 2012). However, there is very limited understanding of the natural variability in
442 Symbiodiniaceae cladal abundance distribution *in hospite*, due to micro-environmental conditions
443 (Wangpraseurt et al. 2014, 2015; Cunning et al. 2015b). By applying the qPCR-HRM assay developed
444 in this study we explored the abundance and repartitioning of Symbiodiniaceae clades at different spatial
445 scales in *A. pulchra*. Our work revealed that the composition of Symbiodiniaceae clade assemblages in
446 this coral species varied at all spatial scales investigated, including geographical (between two sites),
447 inter-colony (within each site), and intra-colony (upward versus downward facing surface of the branch),
448 confirming the high degree of spatial variation in endosymbiotic associations with *Acropora* species
449 (Ulstrup and Van Oppen 2003; Ulstrup et al. 2007; Rouzé et al. 2017).

450 At the geographical scale, significantly higher abundance of total Symbiodiniaceae were
451 observed in *A. pulchra* originating from Mahana compared to Teavaro. The abundance of symbiont
452 types can be enhanced by various environment factors, such as nutrient levels or turbidity (Fabricius
453 2005; Cooper et al. 2011a). The higher total Symbiodiniaceae abundance at the Mahana site, which was
454 characterized by higher turbidity corroborates the findings of Bay et al. (2016) that higher
455 Symbiodiniaceae abundance in corals transplanted to inshore locations which are commonly associated
456 with higher dissolved nutrients. As previously observed in Moorea (Rouzé et al. 2017), up to three
457 distinct clades were detected in a single *A. pulchra* colony, which contrasts with findings of Thomas et
458 al. (2014) who reported exclusive clade C dominance in *A. pulchra* colonies from Western Australia. In
459 the present study, significant differences in the proportion of Symbiodiniaceae clades between sites were
460 observed with a co-dominance of clades A and C in Teavaro compared to multi-clades A and D and
461 clades A, C and D in Mahana. Despite the similar temperatures measured at both sites, (ranging from
462 28.7 to 28.9°C), a higher solar irradiance was recorded at Teavaro (average value: 1767 *vs* 2040 µmol

463 s^{-1} m^2). Coral bleaching is often observed when high temperature and solar irradiance levels occur in
464 combination (Brown and Dunne 2008). It has also been shown that, in addition to the symbiont identity,
465 the abundance of Symbiodiniaceae cells within a coral may play a key role in influencing the function
466 of coral-algal symbiosis, with clade C abundant corals being more prone to bleaching than those with
467 abundant clade D or background C in branched corals (Cunning and Baker 2012; Cunning et al. 2016).
468 As such, the lower total Symbiodiniaceae density observed in the clade C dominated *A. pulchra* colonies
469 from Teavaro (i.e., with higher light levels), could be the result of a mild bleaching event at that location,
470 contrasting with the colonies at Mahana where the putative 'thermo-tolerant' clade D and 'opportunistic'
471 clade A co-dominated and were present at higher densities.

472 Although the broad biological flexibility of *Acropora* sp. to interact with a wide range of
473 Symbiodiniaceae genotypes may be advantageous under stable conditions (see Putnam et al. 2012), the
474 high incidence of clade A reported here in both studied sites may represent a lower resilience potential
475 of coral species from Moorea lagoons. It has been suggested that a higher proportion of clade A in corals
476 could increase their susceptibility to disease and *Vibrio* spp. colonization (Rouzé et al. 2016). The
477 omnipresence of clade A symbionts in *A. pulchra* from both sites is of concern for the health and future
478 of corals in Moorea. Understanding the factors that trigger shifts in Symbiodiniaceae clades abundance
479 and composition in corals around Moorea, through long-term analysis at different spatio-temporal
480 scales, is an interesting avenue for future research.

481 Previous studies (Ulstrup et al. 2007; Kemp et al. 2008, 2014) have described the differential
482 distribution of *in hospite* Symbiodiniaceae clades at the micro-scale (i.e., within a colony), but without
483 taking into account the absolute abundances of each clade and without measuring background symbiont
484 genotypes. Interestingly, 22% of fragments collected from a branch (above *vs* below) of the same colony
485 from Mahana harbored different proportions of Symbiodiniaceae. In this study, micro-scale variations
486 revealed the presence of C-type populations in coral fragments originating from Mahana with lighter
487 colors located below (shaded) compared to the ones located above branches. Although research efforts
488 have focused on revealing the flexibility of coral symbiosis to changing environments and the existence
489 of inter-colony variation among Symbiodiniaceae communities, comparatively little attention has been

given to intra-colony variation. Rowan et al. (1997) emphasized intra-colony zonation of Symbiodiniaceae communities in response to environmental irradiance, suggesting micro-scale physiological acclimatization at the level of colony. Skeletal and tissue properties of corals alter *in hospite* light and oxygen availability to Symbiodiniaceae cells (Wangpraseurt et al. 2014, 2015), creating different niches at the micro-scale and favoring the establishment of different symbiotic clade partnerships that may help corals adapt to the prevailing conditions (Kemp et al. 2008; Suggett et al. 2015). Our study reinforces earlier researches emphasizing the importance of intra-colony variation of Symbiodiniaceae and provides insights into the partitioning of Symbiodiniaceae clades within colonies of *A. pulchra*. Our work highlights the importance of considering micro-niches in studies linking symbiont diversity and coral response to environmental stress to assist in accurately predicting the impact of rising seawater temperature on coral populations and community responses.

In the present study, we developed and validated a qPCR-HRM assay. When coupled with clade and host specific qPCRs, it enabled the absolute quantification of endosymbiotic Symbiodiniaceae from all the nine clades from small coral samples, using the combination of family-Symbiodiniaceae and clades-specific primer sets. The method has the potential to provide useful data on the abundance and repartition of the endosymbiont clades at different biological scales (cells, polyp, colony, population and species), as well as different temporal and spatial scales, which may help understand the drivers behind symbiont community changes (Chen et al. 2005), or those following bleaching events (Thornhill et al. 2006). The method provides a new tool to describe the complexity of coral-Symbiodiniaceae symbiosis in a rapidly changing world. For example, it may contribute to elucidating the mechanisms governing symbiont shuffling as a result of frequent cumulative thermal stress and be useful to quantify horizontal and vertical transmission of symbionts from parental colonies to larvae, thus providing crucial information for restoration applications.

Acknowledgements

This work was funded by the ANR « R-ECOLOGS » and the ANR JCJC « Live and let die ». Sincere thanks are due to Prof. Mary-Alice Coffroth from State University of New York at Buffalo (USA) and Dr. Hollie Putnam from University of Rhode Island (USA) for providing us with Symbiodiniaceae cultures and DNA samples, as well as Dr. Sarah Nahon from French National Institute for Agricultural Research (France) for providing pictures. The authors would like to thank the staff of the CRIOBE for their help during the experiments, and especially Antoine Puisay for his help in sampling corals.

Conflict of Interest:

The authors declare that they have no conflict of interest.

Ethical approval:

All applicable international, national, and/or institutional guidelines for the care and use of animals were followed. Coral collection was performed according to the French Polynesia regulation.

Reference

Arif C, Daniels C, Bayer T, Banguera-Hinestroza E, Barbrook A, Howe CJ, LaJeunesse TC, Voolstra CR (2014) Assessing *Symbiodinium* diversity in scleractinian corals via next-generation sequencing-based genotyping of the ITS2 rDNA region. Mol Ecol 23:4418–4433

Baker AC (2003) Flexibility and specificity in coral-algal symbiosis: Diversity, ccology , and biogeography of *Symbiodinium*. Annu Rev Ecol Evol Syst 34:661–689

Baker AC (2004) Symbiont diversity on coral reefs and its relationship to bleaching resistance and resilience. Corail health and diseases. Springer, pp 177–191

Baker AC, Romanski AM (2007) Multiple symbiotic partnerships are common in scleractinian corals, but not in octocorals: Comment on Goulet (2006). Mar Ecol Prog Ser 335:237–242

Bay LK, Doyle J, Logan M, Berkelmans R (2016) Recovery from bleaching is mediated by threshold densities of background thermo-tolerant symbiont types in a reef-building coral. R Soc Open Sci 3:160322

Berkelmans R, van Oppen MJH (2006) The role of zooxanthellae in the thermal tolerance of corals: a

"nugget of hope" for coral reefs in an era of climate change. Proc R Soc London B Biol Sci 273:2305–2312

Bongaerts P, Frade PR, Ogier JJ, Hay KB, van Bleijswijk J, Englebert N, Vermeij MJA, Bak RPM, Visser PM, Hoegh-Guldberg O (2013) Sharing the slope: depth partitioning of agariciid corals and associated *Symbiodinium* across shallow and mesophotic habitats (2-60 m) on a Caribbean reef. BMC Evol Biol 13:205

Bosserelle P, Berteaux-Lecellier V, Chancerelle Y, Hédouin L, Nugues M, Wallace C, Pichon M (2014) Guide d'identification des coraux de Moorea. CRIOBE.

Boulotte NM, Dalton SJ, Carroll AG, Harrison PL, Putnam HM, Peplow LM, van Oppen MJ (2016) Exploring the Symbiodinium rare biosphere provides evidence for symbiont switching in reef-building corals. ISME J 10:2693–2701

Brown BE, Dunne RP (2008) Solar radiation modulates bleaching and damage protection in a shallow water coral. Mar Ecol Prog Ser 362:99–107

Bustin SA, Benes V, Garson JA, Hellemans J, Huggett J, Kubista M, Mueller R, Nolan T, Pfaffl MW, Shipley GL, Vandesompele J, Wittwer CT (2009) The MIQE guidelines: minimum information for publication of quantitative real-time PCR experiments. Clin Chem 55:611–22

Cantin NE, van Oppen M, Willis BL, Mieog JC, Negri AP, Oppen MJH, Willis BL, Mieog JC, Negri AP (2009) Juvenile corals can acquire more carbon from high-performance algal symbionts. Coral Reefs 28:405–414

Chen CA, Wang J-T, Fang L-S, Yang Y-W (2005) Fluctuating algal symbiont communities in *Acropora palifera* (Scleractinia: Acroporidae) from Taiwan. Mar Ecol Prog Ser 295:113–121

Coffroth MA, Santos SR (2005) Genetic diversity of symbiotic dinoflagellates in the genus *Symbiodinium*. Protist 156:19–34

Cooper TF, Berkelmans R, Ulstrup KE, Weeks S, Radford B, Jones AM, Doyle J, Canto M, O'Leary RA, van Oppen MJH (2011a) Environmental factors controlling the distribution of *Symbiodinium* harboured by the coral *Acropora millepora* on the great barrier reef. PLoS One 6 (10): e25536.

Cooper TF, Ulstrup KE, Dandan SS, Heyward AJ, Kühl M, Muirhead A, O'Leary RA, Ziersen BEF, Van Oppen MJH (2011b) Niche specialization of reef-building corals in the mesophotic zone: metabolic trade-offs between divergent *Symbiodinium* types. Proc R Soc B Biol 278:1840–1850

Cousins MM, Ou S-S, Wawer MJ, Munshaw S, Swan D, Magaret C a, Mullis CE, Serwadda D, Porcella SF, Gray RH, Quinn TC, Donnell D, Eshleman SH, Redd AD (2012) Comparison of a High Resolution Melting (HRM) Assay to Next Generation Sequencing for Analysis of HIV Diversity. J Clin Microbiol 50:3054–3059

Cristescu ME (2014) From barcoding single individuals to metabarcoding biological communities: towards an integrative approach to the study of global biodiversity. Trends Ecol Evol 29:566–571

Cunning R, Baker AC (2012) Excess algal symbionts increase the susceptibility of reef corals to bleaching. Nat Clim Chang 3:259–262

Cunning R, Baker AC (2014) Not just who, but how many: the importance of partner abundance in reef coral symbioses. Front Microbiol 5:400

Cunning R, Ritson-Williams R, Gates R (2016) Patterns of bleaching and recovery of *Montipora capitata* in Kāneʻohe Bay, Hawaiʻi, USA. Mar Ecol Prog Ser 551:131–139

587 Cunning R, Silverstein RN, Baker AC (2015a) Investigating the causes and consequences of symbiont
588 shuffling in a multi-partner reef coral symbiosis under environmental change. Proc R Soc
589 London B Biol Sci 282:20141725

590 Cunning R, Vaughan N, Gillette P, Capo TR, Matté JL, Baker AC, Maté JL, Baker AC (2015b)
591 Dynamic regulation of partner abundance mediates response of reef coral symbioses to
592 environmental change. Ecology 96:1411–20

593 Druml B, Cichna-Markl M (2014) High resolution melting (HRM) analysis of DNA - Its role and
594 potential in food analysis. Food Chem 158:245–254

595 Edmunds PJ, Adjeroud M, Baskett ML, Baums IB, Budd AF, Carpenter RC, Fabina NS, Fan T-Y,
596 Franklin EC, Gross K, Han X, Jacobson L, Klaus JS, McClanahan TR, O'Leary JK, van Oppen
597 MJH, Pochon X, Putnam HM, Smith TB, Stat M, Sweatman H, van Woesik R, Gates RD (2014)
598 Persistence and Change in Community Composition of Reef Corals through Present, Past, and
599 Future Climates. PLoS One 9:e107525

600 Fabricius KE (2005) Effects of terrestrial runoff on the ecology of corals and coral reefs: review and
601 synthesis. Mar Pollut Bull 50:125–146

602 Fitt WK, McFarland FK, Warner ME, Chilcoat GC (2000) Seasonal patterns of tissue biomass and
603 densities of symbiotic dinoflagellates in reef corals and relation to coral bleaching. Limnol
604 Oceanogr 45:677–685

605 Goulet TL (2007) Most scleractinian corals and octocorals host a single symbiotic zooxanthella clade.
606 Mar Ecol Prog Ser 335:243–248

607 Granados-Cifuentes C, Rodriguez-Lanetty M (2011) The use of high-resolution melting analysis for
608 genotyping *Symbiodinium* strains: a sensitive and fast approach. Mol Ecol Resour 11:394–399

609 Hédouin L, Pilon R, Puisay A (2015) Hyposalinity stress compromises the fertilization of gametes
610 more than the survival of coral larvae. Mar Environ Res 104:1–9

611 Hellemans J, Mortier G, De Paepe A, Speleman F, Vandesompele J (2007) qBase relative
612 quantification framework and software for management and automated analysis of real-time
613 quantitative PCR data. Genome Biol 8:R19

614 Hoegh-Guldberg O, Mumby PJ, Hooten AJ, Steneck RS, Greenfield P, Gomez E, Harvell CD, Sale
615 PF, Edwards AJ, Caldeira K (2007) Coral reefs under rapid climate change and ocean
616 acidification. Science (80) 318:1737

617 Howells EJ, Beltran VH, Larsen NW, Bay LK, Willis BL, van Oppen MJH (2012) Coral thermal
618 tolerance shaped by local adaptation of photosymbionts. Nat Clim Chang 2:116–120

619 Howells EJ, Willis BL, Bay LK, Van Oppen MJH (2013) Spatial and temporal genetic structure of
620 Symbiodinium populations within a common reef-building coral on the Great Barrier Reef. Mol
621 Ecol 22:3693–3708

622 Hughes TP, Baird AH, Bellwood DR, Card M, Connolly SR, Folke C, Grosberg R, Hoegh-Guldberg
623 O, Jackson JBC, Kleypas JA, Lough JM, Marshall P, Nyström M, Palumbi SR, Pandolfi JM,
624 Rosen B, Roughgarden J, Nystrom M (2003) Climate change, human impacts, and the resilience
625 of coral reefs. Science (80) 301:929–933

626 Hughes TP, Kerry JT, Álvarez-Noriega M, Álvarez-Romero JG, Anderson KD, Baird AH, Babcock
627 RC, Beger M, Bellwood DR, Berkelmans R, Bridge TC, Butler IR, Byrne M, Cantin NE,
628 Comeau S, Connolly SR, Cumming GS, Dalton SJ, Diaz-Pulido G, Eakin CM, Figueira WF,
629 Gilmour JP, Harrison HB, Heron SF, Hoey AS, Hobbs J-PA, Hoogenboom MO, Kennedy E V,
630 Kuo C, Lough JM, Lowe RJ, Liu G, McCulloch MT, Malcolm HA, McWilliam MJ, Pandolfi

631 JM, Pears RJ, Pratchett MS, Schoepf V, Simpson T, Skirving WJ, Sommer B, Torda G,
632 Wachenfeld DR, Willis BL, Wilson SK (2017) Global warming and recurrent mass bleaching of
633 corals. Nature 543:373–377

634 Hume BCC, D'Angelo C, Smith EG, Stevens JR, Burt J, and Wiedenmann J. 2015. *Symbiodinium*
635 *thermophilum* sp nov., a thermotolerant symbiotic alga prevalent in corals of the world's hottest
636 sea, the Persian/Arabian Gulf. Scientific Reports 5:08562

637 Hume BCC, Ziegler M, Poulain J, Pochon X, Romac S, Boissin E, de Vargas C, Planes S, Wincker P,
638 Voolstra CR (2018) An improved primer set and amplification protocol with increased
639 specificity and sensitivity targeting the *Symbiodinium* ITS2 region. PeerJ 6:e4816.

640 Jones AM, Berkelmans R, van Oppen MJH, Mieog JC, Sinclair W (2008) A community change in the
641 algal endosymbionts of a scleractinian coral following a natural bleaching event: field evidence
642 of acclimatization. Proc R Soc B Biol 275:1359–1365

643 Kemp DW, Fitt WK, Schmidt GW (2008) A microsampling method for genotyping coral symbionts.
644 Coral Reefs 27:289–293

645 Kemp DW, Hernandez-Pech X, Iglesias-Prieto R, Fitt WK, Schmidt GW (2014) Community dynamics
646 and physiology of *Symbiodinium* spp. before, during, and after a coral bleaching event. Limnol
647 Ocean 59:788–797

648 Kennedy E V, Tonk L, Foster NL, Chollett I, Ortiz J-C, Dove S, Hoegh-Guldberg O, Mumby PJ,
649 Stevens JR (2016) *Symbiodinium* biogeography tracks environmental patterns rather than host
650 genetics in a key Caribbean reef-builder, *Orbicella annularis*. Proc R Soc B Biol Sci 283:
651 20161938.

652 LaJeunesse TC, Smith R, Walther M, Pinzón J, Pettay DT, McGinley M, Aschaffenburg M, Medina-
653 Rosas P, Cupul-Magaña AL, Pérez AL, Reyes-Bonilla H, Warner ME (2010) Host-symbiont
654 recombination versus natural selection in the response of coral-dinoflagellate symbioses to
655 environmental disturbance. Proc Biol Sci 277:2925–2934

656 LaJeunesse TC, Parkinson JE, Gabrielson PW, Jeong HJ, Reimer JD, Voolstra CR, Santos SR
657 (2018). Systematic revision of Symbiodiniaceae highlights the antiquity and diversity of coral
658 endosymbionts. Curr Biol 28:1-11

659 Lavergne E, Calves I, Meistertzheim AL, Charrier G, Zajonz U, Laroche J (2014) Complex genetic
660 structure of a euryhaline marine fish in temporarily open/closed estuaries from the wider Gulf of
661 Aden. Mar Biol 161:113–1126

662 Little AF, van Oppen MJH, Willis BL (2004) Flexibility in Algal Endosymbioses Shapes Growth in
663 Reef Corals. Science (80-) 304:1492–1494

664 Loram JE, Boonham N, O'Toole P, Trapido-Rosenthal HG, Douglas AE (2007) Molecular
665 quantification of symbiotic dinoflagellate algae of the genus *Symbiodiniu*m. Biol Bull 212:259–
666 68

667 Marshall SM (1932) Notes on oxygen production in coral planulae. Grt Barrier ReefExped Sci Rep
668 1:253–258

669 McGinley MP, Aschaffenburg MD, Pettay DT, Smith RT, LaJeunesse TC, Warner ME (2012)
670 *Symbiodinium* spp. in colonies of eastern Pacific *Pocillopora* spp. are highly stable despite the
671 prevalence of low-abundance background populations. Mar Ecol Prog Ser 462:1–7

672 Meistertzheim A-L, Calves I, Artigaud S, Friedman CS, Laroche J, Paillard C, Ferec C (2012) High
673 Resolution Melting Analysis for fast and cheap polymorphism screening of marine populations.

674 Protoc Exch doi:10.1038/protex.2012.015

675 Mieog JC, Van Oppen MJH, Berkelmans R, Stam WT, Olsen JL (2009) Quantification of algal
676 endosymbionts (*Symbiodinium*) in coral tissue using real-time PCR. Mol Ecol Resour 9:74–82

677 Mieog JC, van Oppen MJH, Cantin NE, Stam WT, Olsen JL (2007) Real-time PCR reveals a high
678 incidence of *Symbiodinium* clade D at low levels in four scleractinian corals across the Great
679 Barrier Reef: implications for symbiont shuffling. Coral Reefs 26:449–457

680 National Oceanic and Atmospheric Administration N (2016) "NOAA Declares Third Ever Global
681 Coral Bleaching Event." Oct. 2015. Web. 12 Jan. 2016.

682 Naue J, Hansmann T, Schmidt U (2014) High-resolution melting of 12S rRNA and cytochrome b
683 DNA sequences for discrimination of species within distinct European animal families. PLoS
684 One 9:e115575

685 Pfaffl MW (2001) A new mathematical model for relative quantification in real-time RT–PCR.
686 Nucleic Acids Res 29:2003–2007

687 Pettay, D. T., and Lajeunesse, T. C. (2013). Long-range dispersal and high-latitude environments influence
688 the population structure of a "stress-tolerant" dinoflagellate endosymbiont. PLoS One 8:e79208.

689 Pochon X, Gates RD (2010) A new *Symbiodinium* clade (Dinophyceae) from soritid foraminifera in
690 Hawai'i. Mol Phylogenet Evol 56:492–497

691 Pochon X, Putnam HM, Gates RD (2014) Multi-gene analysis of *Symbiodinium* dinoflagellates: a
692 perspective on rarity, symbiosis, and evolution. PeerJ 2:e394

693 Putnam HM, Stat M, Pochon X, Gates RD (2012) Endosymbiotic flexibility associates with
694 environmental sensitivity in scleractinian corals. Proc R Soc B Biol 279:4352–4361

695 Quigley KM, Davies SW, Kenkel CD, Willis BL, Matz M V., Bay LK (2014) Deep-sequencing
696 method for quantifying background abundances of *Symbiodinium* types: Exploring the rare
697 *Symbiodinium* biosphere in reef-building corals. PLoS One 9(4): e94297

698 Reaka-Kudla ML (1997) The global biodiversity of coral reefs: a comparison with rain forests. In: (ed)
699 R.-K. et al. (eds) Biodiversity II: Understanding and Protecting our biological resources. National
700 Academy Press, Joseph Henry Press, pp 83–108

701 Rouzé H, Lecellier G, Saulnier D, Berteaux-Lecellier V (2016) *Symbiodinium* clades A and D
702 differentially predispose *Acropora cytherea* to disease and *Vibrio* spp. colonization. Ecol Evol
703 6:560–572

704 Rouzé H, Lecellier GJ, Saulnier D, Planes S, Gueguen Y, Wirshing HH, Berteaux-Lecellier V (2017)
705 An updated assessment of *Symbiodinium* spp. that associate with common scleractinian corals
706 from Moorea (French Polynesia) reveals high diversity among background symbionts and a
707 novel finding of clade B. PeerJ 5:e2856

708 Rowan R (2004) Coral Bleaching:Thermal adaptation in reef coral symbionts. Nature 430:742

709 Rowan R, Knowlton N (1995) Intraspecific diversity and ecological zonation in coral-algal symbiosis.
710 Proc Natl Acad Sci 92:2850–2853

711 Rowan R, Knowlton N, Baker A, Jara J (1997) Landscape ecology of algal symbionts creates variation
712 in episodes of coral bleaching. Nature 388:265–269

713 Santos SR, Coffroth MA (2003) Molecular genetic evidence that dinoflagellates belonging to the
714 genus *Symbiodinium* Freudenthal are haploid. Biol Bull 204:10–20

715 Silverstein RN, Correa AMS, Baker AC (2012) Specificity is rarely absolute in coral-algal symbiosis:
716 implications for coral response to climate change. Proc R Soc B Biol Sci 279:2609–2618

717 Spalding M, Ravilious C, Green E (2001) World Atlas of Coral Reefs. University of California Press
718 and UNEP/WCMC, Berkeley, CA

719 Spalding MD, Grenfell AM (1997) New estimates of global and regional coral reef areas. Coral Reefs
720 16:225–230

721 Stat M, Baker AC, Bourne DG, Correa AMS, Forsman Z, Huggett MJ, Pochon X, Skillings D, Toonen
722 RJ, van Oppen MJH, Gates RD (2012) Molecular Delineation of Species in the Coral Holobiont.
723 Adv Mar Biol 63:1–65

724 Stat M, Carter D, Hoegh-Guldberg O (2006) The evolutionary history of *Symbiodinium* and
725 scleractinian hosts--Symbiosis, diversity, and the effect of climate change. Perspect Plant Ecol
726 Evol Syst 8:23–43

727 Stat M, Gates RD (2011) Clade D *Symbiodinium* in Scleractinian Corals: A "Nugget" of Hope, a
728 Selfish Opportunist, an Ominous Sign, or All of the Above? J Mar Biol 2011:1–9

729 Stat M, Morris E, Gates RD (2008) Functional diversity in coral–dinoflagellate symbiosis. PNAS
730 105:9256

731 Suggett DJ, Goyen S, Evenhuis C, Szabó M, Pettay DT, Warner ME, Ralph PJ (2015) Functional
732 diversity of photobiological traits within the genus *Symbiodinium* appears to be governed by the
733 interaction of cell size with cladal designation. New Phytol 208:370–381

734 Tamura K, Stecher G, Peterson D, Filipski A, Kumar S (2013) MEGA6: Molecular Evolutionary
735 Genetics Analysis Version 6.0. Mol Biol Evol 30:2725–2729

736 Thomas L, Kendrick GA, Kennington WJ, Richards ZT, Stat M (2014) Exploring *Symbiodinium*
737 diversity and host specificity in *Acropora* corals from geographical extremes of Western
738 Australia with 454 amplicon pyrosequencing. Mol Ecol 23:3113–26

739 Thornhill DJ, LaJeunesse TC, Kemp DW, Fitt WK, Schmidt GW (2006) Multi-year, seasonal
740 genotypic surveys of coral-algal symbioses reveal prevalent stability or post-bleaching reversion.
741 Mar Biol 148:711–722

742 Thornhill DJ, Xiang Y, Fitt WK, Santos SR (2009) Reef endemism, host specificity and temporal
743 stability in populations of symbiotic dinoflagellates from two ecologically dominant Caribbean
744 corals. PLoS One 4:e6262

745 Thornhill, D. J., Howells, E. J., Wham, D. C., Steury, T. D., and Santos, S. R. (2017). Population genetics
746 of reef coral endosymbionts (*Symbiodinium*, Dinophyceae). Mol. Ecol. 26, 2640–2659
747
748 Tonk L, Sampayo EM, LaJeunesse TC, Schrameyer V, Hoegh-Guldberg O (2014) *Symbiodinium*
749 (Dinophyceae) diversity in reef-invertebrates along an offshore to inshore reef gradient near
750 Lizard Island, Great Barrier Reef. J Phycol 50:552–563

751 Ulstrup KE, Van Oppen MJH (2003) Geographic and habitat partitioning of genetically distinct
752 zooxanthellae (*Symbiodinium*) in *Acropora* corals on the Great Barrier Reef. Mol Ecol 12:3477–
753 3484

754 Ulstrup KE, Van Oppen MJH, Kühl M, Ralph PJ (2007) Inter-polyp genetic and physiological
755 characterisation of *Symbiodinium* in an *Acropora valida* colony. Mar Biol 153:225–234

756 Wangpraseurt D, Pernice M, Guagliardo P, Kilburn MR, Clode PL, Polerecky L, Kuhl M (2015) Light
757 microenvironment and single-cell gradients of carbon fixation in tissues of symbiont-bearing

758 corals. ISME J 10:788–792

759 Wangpraseurt D, Polerecky L, Larkum AWD, Ralph PJ, Nielsen DA, Pernice M, Kühl M (2014) The
760 in situ light microenvironment of corals. Limnol Oceanogr 59:917–926

761 Wilkinson C (2000) Status of Coral Reefs of the World 2000. Australian Institute of Marine Science,
762 Townsville, Australia, 557pp

763 Wittwer CT, Reed GH, Gundry CN, Vandersteen JG, Pryor RJ (2003) High-Resolution Genotyping by
764 Amplicon Melting Analysis Using LCGreen. Clin Chem 49:853–860

765 Yuan JS, Reed A, Chen F, Stewart Jr. CN, Stewart Jr CN (2006) Statistical analysis of real-time PCR
766 data. BMC Bioinformatics 7:85–97

767

768

769 **Author contribution**

770 A.L.M., and L.H. designed research; A.L.M. performed research; A.L.M. and X.P. analyzed data;
771 A.L.M. and X.P. wrote the paper; and J.F.G., S.A.W. and L.H. revised the paper.

772 **Additional Information**

773 The authors declare no conflict of interest.

774

775 **Figure legend**

776 **Figure S1** Alignment of 5.8S rDNA partial sequences corresponding to the nine existing
777 Symbiodiniaceae clades extracted from Pochon et al., (2014) used for HRM-primer set design.

778 **Figure S2** Linear regressions derived from DNAs extracted from 1×10^3 to 3×10^6 Symbiodiniaceae cells
779 per extraction (A), and for 2 to 400 cells per extraction of *Acropora pulchra* embryos (B).

780 **Figure 1** Sampling locations and the host sampling strategy used to investigate the fine-scale assemblage
781 of Symbiodiniaceae phylogenetic clades in different colonies of *Acropora pulchra* from: (A) Moorea
782 Island (French Polynesia, South-Pacific), and (B) at the two sampling sites of Mahana and Teavaro.
783 *Acropora pulchra* type colony at Mahana (C), and (D) the pictorial description of the design used to
784 sample the normal (N) and slightly bleached (sB) fragments of colonies.

785 **Figure 2** Linear section of the standard curves obtained for the quantification of Symbiodiniaceae cells
786 using the clade-specific (blue) and genus-generalist Symbiodiniaceae primers (green) for a range of
787 1×10^3 to 3×10^6 cells (A). Standard curve obtained for the quantification of host cells corresponding to a
788 range of 2 to 400 *Acropora pulchra* cells (B).

789 **Figure 3** Melt curves and root-mean square error (RMSE) values for the Symbiodiniaceae clade-specific
790 qPCR-High Resolution Melt (HRM) assay. (*a*) Normalized HRM results using the 5.8S rRNA gene and
791 DNA samples belonging to Symbiodiniaceae clades A to I. (*b*) Melting peaks derived from the
792 normalized HRM curves presented in A. (*c*) Mean RMSE value (±SD) for the pairwise comparisons of

793 normalized HRM curves between clades presented in a). Dotted line represented the mean RMSE value
794 obtained for pairwise comparisons within clades.

795 **Figure 4** Melting peaks using the 5.8S rRNA gene from mixtures observed in samples (solid line) and
796 *in vitro* mixtures (dotted line) combining two clades (*a*) or three clades (*b*), and clade A and D at different
797 proportions (*c*). Reference melting curves of each clade are shown in grey.

798 **Figure 5** Cellular proportions of specific Symbiodiniaceae clades per total DNA (Symbiodiniaceae +
799 host) measured *via* qPCR- High Resolution Melt for both normal (N) and slightly bleached (sB)
800 fragments of *Acropora pulchra* colonies sampled at the Mahana and Teavaro sites.

801 **Figure 6** Means proportions and standard deviations (SD) of specific Symbiodiniaceae clades per total
802 DNA (Symbiodiniaceae + host) for normal (N) and slightly bleached (sB) fragments of *Acropora*
803 *pulchra* colonies sampled at the Mahana and Teavaro sites. *significant differences at $p<0.05$,
804 **significant differences at $p<0.01$, ***significant differences at $p<0.001$.

805

806 **Table 1**. Combinations of forward and reverse primers used in real-time PCR and High
807 Resolution Melting analyses.

808

Figure 1

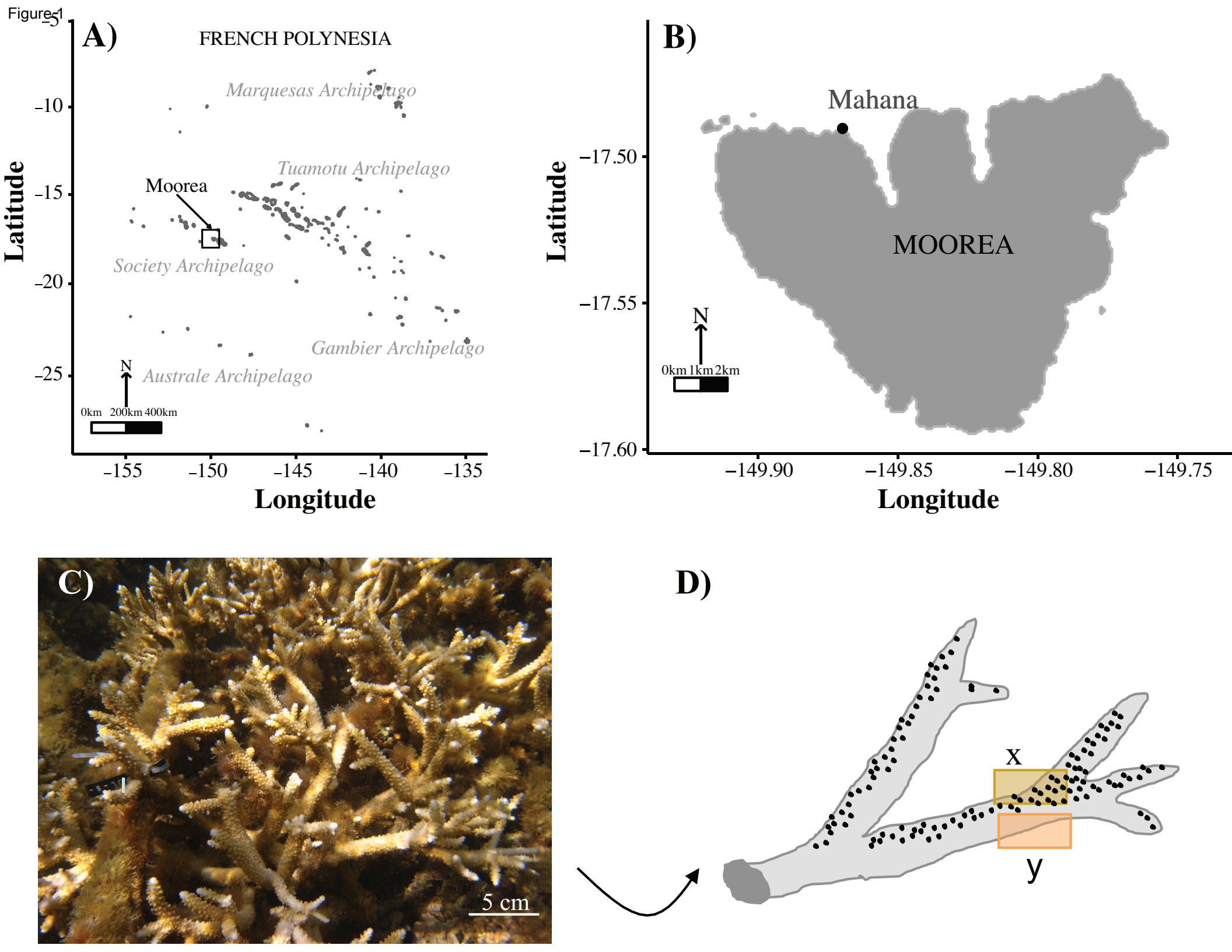
A)
FRENCH POLYNESIA
Marquesas Archipelago
Tuamotu Archipelago
Moorea
Society Archipelago
Gambier Archipelago
Australe Archipelago
N
0km 200km 400km
Latitude
Longitude
-5
-10
-15
-20
-25
-155
-150
-145
-140
-135
B)
Mahana
MOOREA
N
0km 1km 2km
Latitude
Longitude
-17.50
-17.55
-17.60
-149.90
-149.85
-149.80
-149.75
C)
5 cm
D)
X
y

Figure 2

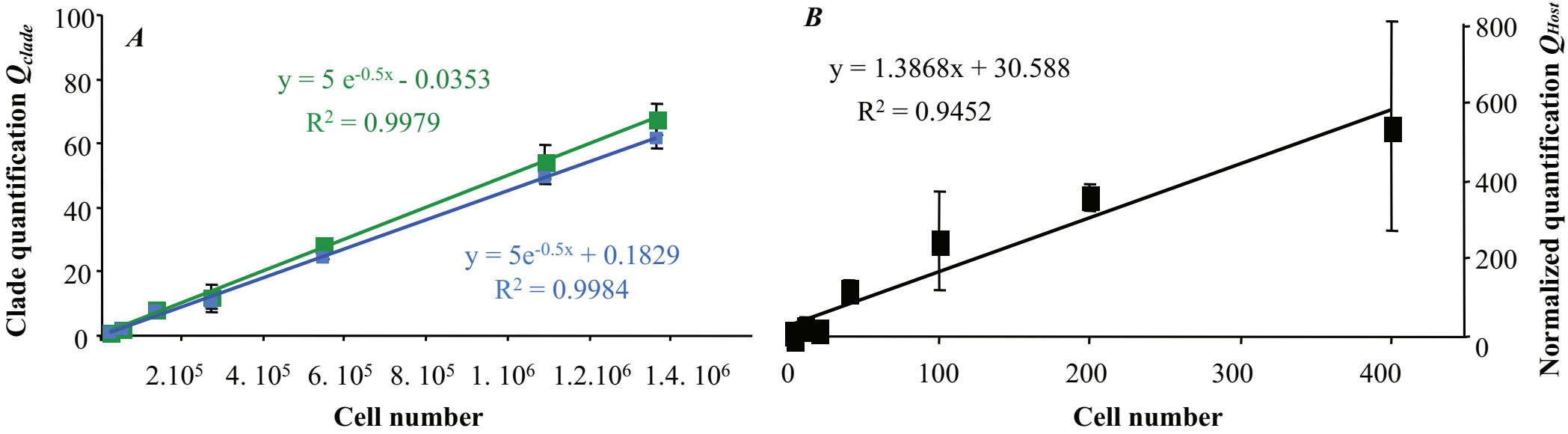
A
y = 5 e-0.5x - 0.0353
R2 = 0.9979
y = 5e-0.5x + 0.1829
R2 = 0.9984
Clade quantification Qclade
Cell number
B
y = 1.3868x + 30.588
R2 = 0.9452
Normalized quantification QHost
Cell number

Figure 3

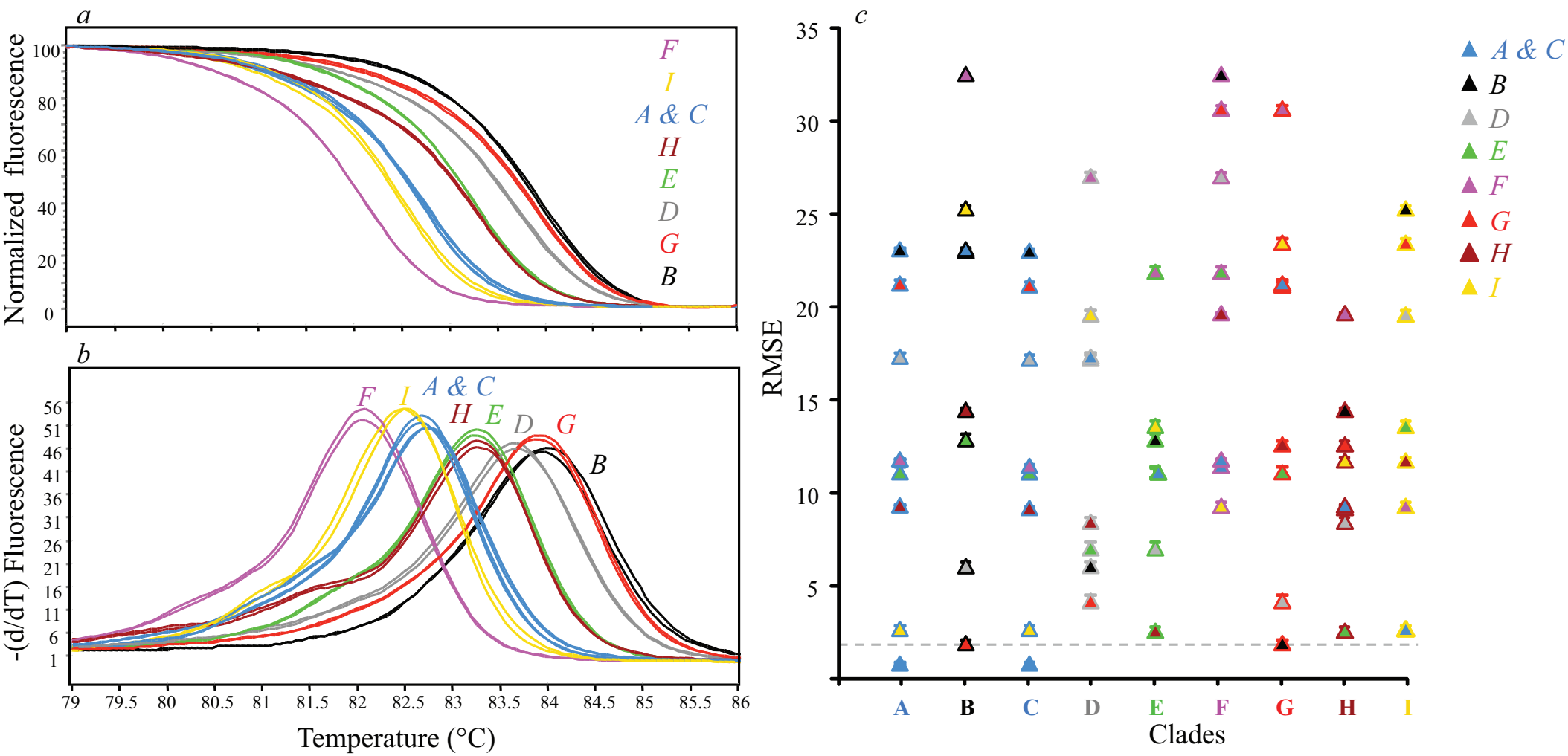
a
Normalized fluorescence
100
80
60
40
20
0
F
I
A & C
H
E
D
G
B
b
-(d/dT) Fluorescence
56
51
46
41
36
31
26
21
16
11
6
1
F
I
A & C
H
E
D
G
B
79
79.5
80
80.5
81
81.5
82
82.5
83
83.5
84
84.5
85
85.5
86
Temperature (°C)
c
RMSE
35
30
25
20
15
10
5
A & C
B
D
E
F
G
H
I
A
B
C
D
E
F
G
H
I
Clades

Figure 4

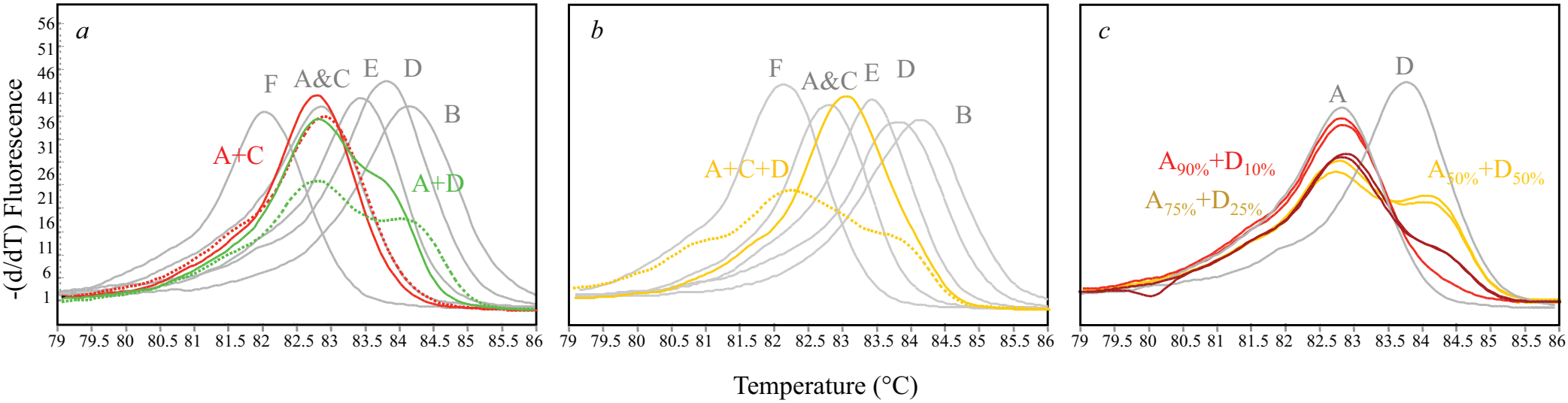
a
b
c
F
A&C
E
D
B
A
A+C
A+D
A+C+D
A90%+D10%
A75%+D25%
A50%+D50%
-(d/dT) Fluorescence
Temperature (°C)
56
51
46
41
36
31
26
21
16
11
6
1
79
79.5
80
80.5
81
81.5
82
82.5
83
83.5
84
84.5
85
85.5
86

Figure 5

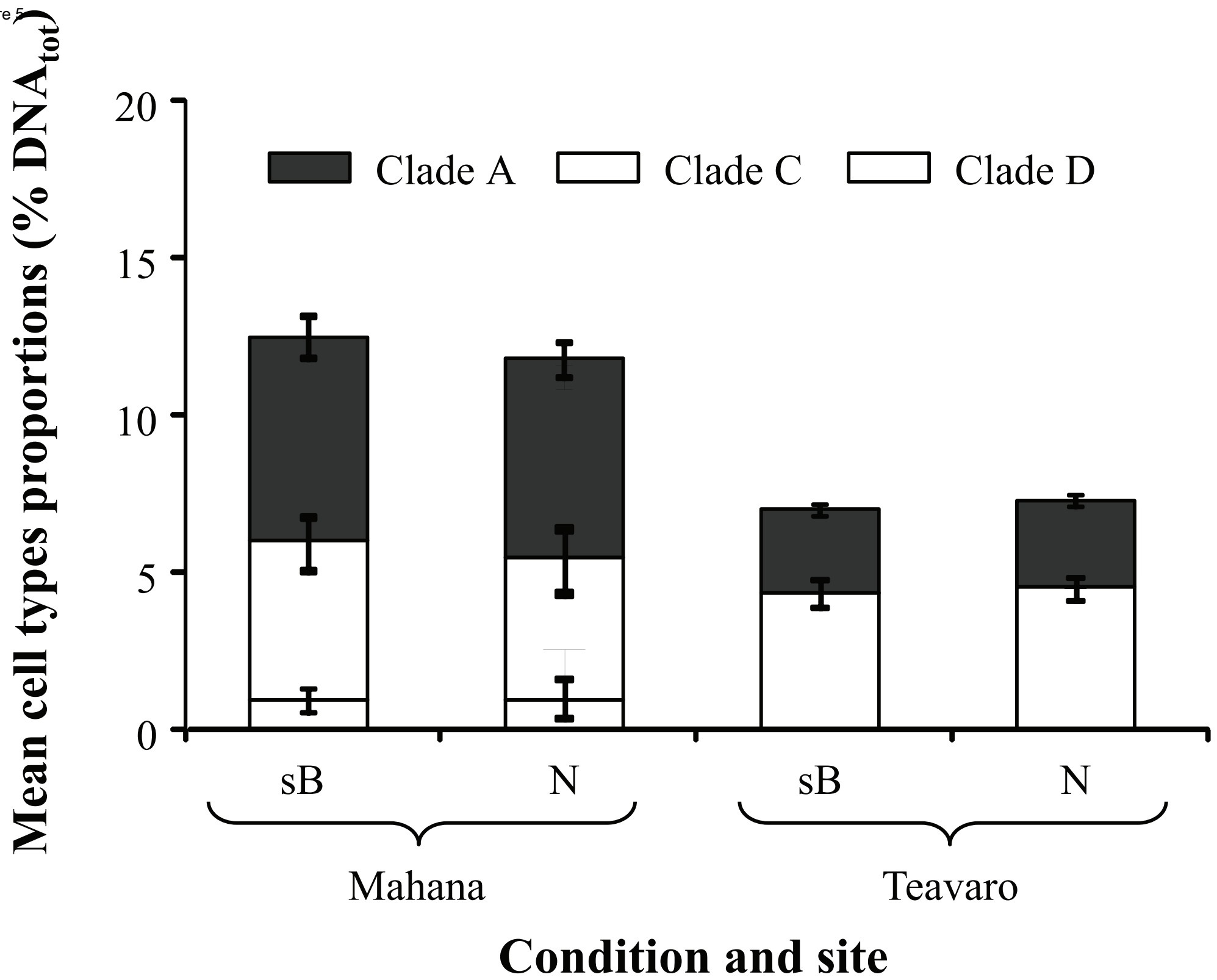
Mean cell types proportions (% DNAtot)
20
15
10
5
0
Clade A
Clade C
Clade D
sB
N
sB
N
Mahana
Teavaro
Condition and site

Figure 6

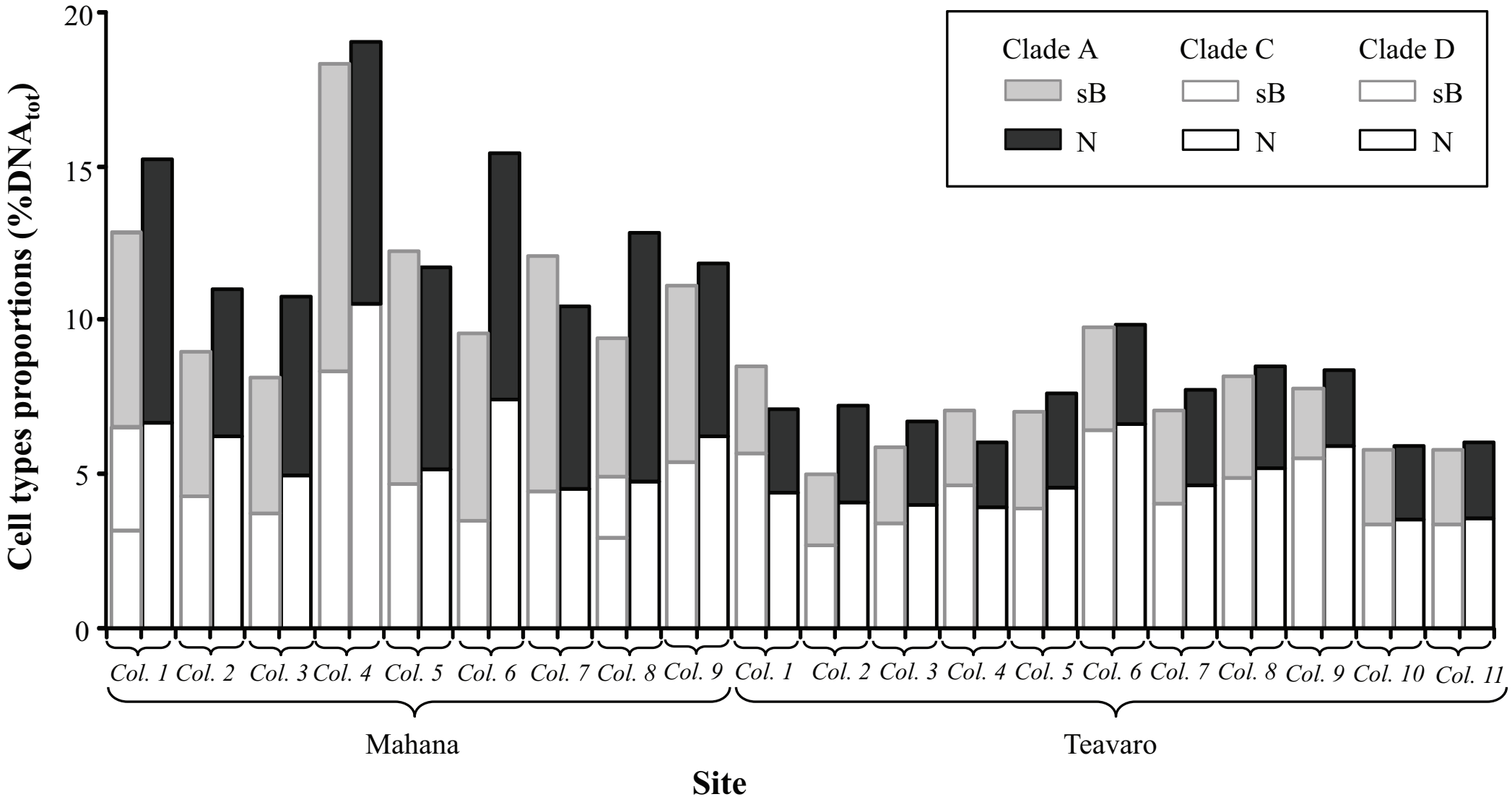
Clade A
sB
N
Clade C
sB
N
Clade D
sB
N
Cell types proportions (%DNA$_{tot}$)
20
15
10
5
0
Col. 1 Col. 2 Col. 3 Col. 4 Col. 5 Col. 6 Col. 7 Col. 8 Col. 9
Col. 1 Col. 2 Col. 3 Col. 4 Col. 5 Col. 6 Col. 7 Col. 8 Col. 9 Col. 10 Col. 11
Mahana
Teavaro
Site

Table 1. Combinations of forward and reverse primers used in real-time PCR and High Resolution Melting analyses.

Specificity	Target gene	Primer Names Forward / Reverse	Forward (5'-3')	Reverse (5'-3')	Amplicon size (bp)	Efficiency	Reference
Symbiont							
Symbiodiniacea	5.8S	SYM_VAR_5.8S2 / Symb_R	GAATTGCAGAACTCCGTGAACC	AGCACTGAAGCAGACATACTCTCAG	80	2	Hume et al. (2015) / This study
Clade A	ITS2	Aits2_F / Aits2_R	AGCAGTGCTGCTGCATGCT	TGTCTGACTTCATGCTAGGAAGTGTT	148	1,93	This study
Clade B	ITS2	Bits2_F / Bits2_F	TTCCAACAAGTCATCGATCGC	TGGCGCATGGGCCA	65	1,88	This study
Clade C	Actin	Cact_F / Cact_R	CCAGGTGCGATGTCGATATTC	TGGTCATTCGCTCACCAATG	96	2,02	Cunning and Baker (2012)
Clade D	Actin	Dact_F / Dact_R	GGCATGGGGTAAGCACTTCTT	GATCCTTGAACTAGCCTTGGAAAC	106	1,96	Cunning and Baker (2012)
Clade E	ITS2	Eits2_F / Eits2_R	TTCCTGGAGAAGCCTTGAG	AGCTTACCTCCCGGTTTGTGTT	83	1,84	This study
Clade F	ITS2	Fits2_F / Fits2_R	GCCCCTGTGAGCCATTGA	AAGGTGGAATCTTGAATAGAAGCG	91	1,85	This study
Clade G	ITS2	Gits2_F / Gits2_R	GCCTCGGCGTGTTGTTG	AGCACGTGCATGCTTGCA	72	2	This study
Clade H	ITS2	Hits2_F / Hits2_R	CCTGCTTTTTGCGTTCCTATG	ACTCAAGCAAAGCCGTGCA	122	2	This study
Clade I	ITS2	Iits2_F / Iits2_R	ACTCCTGCAAGCCATCGCT	TTGCTATGAATCACAAAGCGCT	90	2	This study
Host							
Acropora pulchra	Actin	Actin_F / Actin_R	ATCATGAAGTGCGATGTGGACA	CTGCATTCTGTCAGCGATTCC	99	2,01	This study
Acropora pulchra	5.8S	5.8S_F / 5.8S_R	CCGGTGGATCTCTTGGCTC	CGCCATTTGCGTTCAAAGA	107	1,99	This study

Electronic Supplementary Material (Tables, Figures, Video, Movie, Audio, etc.)